JOURNAL OF SPACECRAFT AND ROCKETS
Vol. 42, No. 4, July–August 2005

Lidar Backscatter Properties of Al_2O_3 Rocket Exhaust Particles

Robert A. Reed* and Mitchel K. Nolen†
Jacobs—Sverdrup Corporation, Arnold Air Force Base, Tennessee 37389
Michael E. Zolensky‡
NASA Johnson Space Center, Houston, Texas 77058
Isaac Bankman,‡ John Giles,‡ and Peter Lang§
Johns Hopkins University, Applied Physics Laboratory, Laurel, Maryland 20723
Michael I. Mishchenko¶
NASA Goddard Institute for Space, New York, New York 10025
and
Martin N. Ross**
The Aerospace Corporation El Segundo, California 90009

The lidar backscatter cross sections of aluminum-oxide rocket exhaust particles are sensitive to slight deviations from their nominal spherical shape. We have therefore determined the distribution of particle shapes using automated image analysis of scanning electron microscope particle photographs. These shape statistics were used in conjunction with T-matrix calculations for nonspherical particles to estimate the backscatter properties of representative rocket exhaust particles. For the range of particle sizes and nonsphericities ε relevant to exhaust plumes, both the backscatter intensity and depolarization scale approximately with the product of nonsphericity ε times the particle radius (εr). This correlation allows us to formulate a simple model for both the backscatter intensity and the depolarization of typical Al_2O_3 rocket exhaust particles. This model is applied to a recent particle collection from the exhaust plume of a Titan-IVA rocket obtained from the NASA WB-57F high-altitude research aircraft at an altitude of 19 km.

I. Introduction

LIDAR has been used as a means to track rocket exhaust plumes and also to characterize the size of exhaust particles from aluminized solid-propellant rocket motors such as the space shuttle. Traditionally, lidar backscatter cross sections for Al_2O_3 rocket particles have been computed assuming homogeneous spheres using Mie theory.[1–4] This is based upon the approximately spherical shape observed for typical particles. However, because backscatter is extremely sensitive to particle shape, the use of Mie theory is suspect. As a first step towards developing a more realistic description of rocket exhaust plume backscatter, we determined the shapes of 145 high-quality scanning electron microscope particle images collected from a variety of sources, including the space shuttle launchpad and the NASA high-altitude U-2, ER-2, and WB-57 aircraft.[5–10] We then used this information to evaluate the backscatter cross section using the observed distribution of shapes and a T-Matrix code for nonspherical particle scattering.

II. Properties of Rocket Particles

The principal source of scattering in aluminized solid-propellant rocket exhaust plumes is Al_2O_3 (aluminum-oxide) particles. The mass-mean radii of Al_2O_3 particles in upper-stage II and III booster rocket motor exhausts are believed to be in the range 2–4 μm (Refs. 2 and 10–13). Al_2O_3 is a reflective dielectric material,[14] and as expected, plumes composed of Al_2O_3 particles give strong lidar returns. Figure 1 shows a representative scanning electron microscope photograph of an Al_2O_3 rocket exhaust particle collected from the high-altitude NASA ER-2 and WB-57.[5–9,13] Although one can occasionally find an almost perfectly round particle, most exhibit minor deviations from ideal spherical symmetry. The nature of heterogeneous aluminum combustion in the motor chamber and the existence of multiple crystal phases of solid Al_2O_3 (Refs. 15 and 16) also suggest the likelihood of internal inhomogeneities, voids, and refractive index gradients within the volume of the particle. Even if these do not affect the outward shape, they will still cause the particle to scatter laser light in a nonspherical manner. Minor imperfections like the ones shown in Fig. 1 will have little effect upon the emissivity and the total scattering cross section. However, they will significantly reduce the backscatter cross section and will radically alter the polarization state of the scattered light, hence our interest in particle shape. Figure 2 shows a statistical analysis of particle shape determined by a computerized image analysis (ImagePro-V®) of 145 particles collected from several sources. The observed nonsphericities $\varepsilon = (D_{MAX} - D_{MIN})/2D_{AVG}$ are generally between 2–5%. In the past, this small degree of nonsphericity was appealed to to justify the use of Mie theory to predict the particle backscatter properties. However, as will be shown, this is inaccurate for the intensity of the backscatter and grossly incorrect for the polarization.

III. Model for Backscatter

T-matrix codes for nonspherical particles have progressed to the point where calculations for mildly nonspherical particles with size parameters in excess of 100 are now possible, including the effects of orientational averaging.[17] In this paper we use a refractive index $m = 1.75 + 0.0005i$ and the wavelength $\lambda = 532$ nm. However, the refractive index of Al_2O_3 varies slowly enough with wavelength so that these results are also applicable to the commonly used 1064-nm fundamental and 355-nm third-harmonic wavelengths of the Nd:YAG laser as well, provided that one expresses the scattering functions in terms of the dimensionless size parameter rather than in terms of the absolute size. Figure 3 shows an example of the

Received 12 January 2004; revision received 25 June 2004; accepted for publication 11 August 2004.

*Senior Scientist, AEDC Group.
†Senior Engineer, AEDC Group.
‡Senior Scientist.
§Senior Programmer.
¶Senior Scientist, Institute for Space Studies.
**Director, Launch Systems Studies.

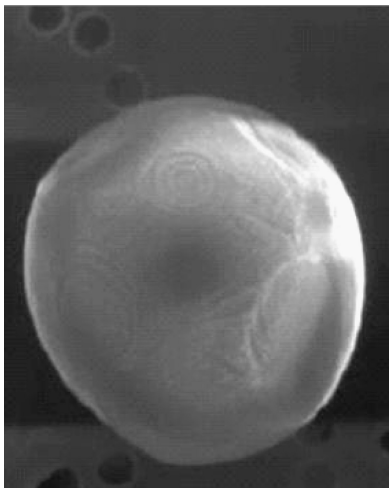

Fig. 1 A 3.5-μm-diam Al_2O_3 stratospheric rocket exhaust particle.

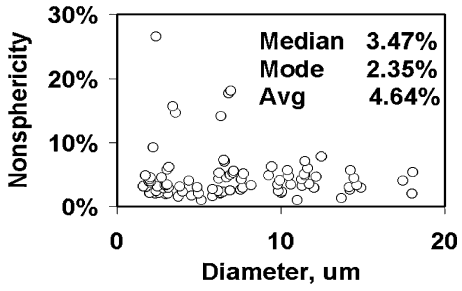

Fig. 2 Particle shape statistics.

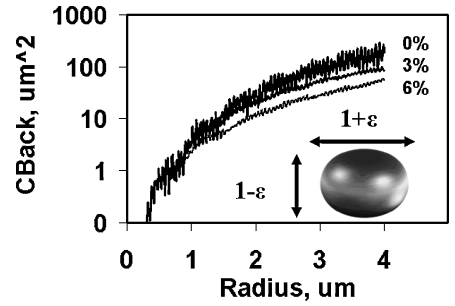

Fig. 3 Backscatter intensity from spheroids.

backscatter intensity from spheroids of increasing nonsphericity ε, identified by the percentages in the legend. A nonsphericity of 0% corresponds to an ideal sphere. The effect of increasing nonsphericity is to decrease the overall amplitude of the backscatter and to suppress the fine-scale oscillatory "interference structure" characteristic of a sphere.

The polarization state of light is specified by the four-component Stokes vector and the associated 4×4 scattering (or Mueller) matrix. We use the [I, Q, U, V] notation of Bohren and Huffman.[18] Equation (1) shows that regardless of particle shape, the scattering matrix assumes a particularly simple form in the 180-deg backscatter direction when the particles are randomly oriented[19,20]:

$$S_{ij}(180) = S_{11} \cdot \begin{bmatrix} 1 & 0 & 0 & \delta \\ 0 & 1-\Delta & 0 & 0 \\ 0 & 0 & -(1-\Delta) & 0 \\ \delta & 0 & 0 & 1-2\cdot\Delta \end{bmatrix} \quad (1)$$

where S_{11} is an abbreviation for $S_{11}(180)$, and where the depolarization factor $\Delta = 1 - S_{11}(180)/S_{22}(180)$ (Ref. 18). The backscatter depolarization ratio (HV/VV) corresponding to Δ is $= \Delta/(2-\Delta)$. $\Delta = 0$ for spheres, and $\delta = 0$ for any particle shape that has mirror symmetry (e.g., spheres, ellipsoids, and any shape with rotational symmetry). The off-diagonal term δ is related to the "handedness" (left handed vs right handed) of the particles and the interconversion of circular and linear polarized light. Laboratory measurements of irregularly shaped particles in water suspension[21] and in aerosol form[22,23] indicate that, when averaged over a particle shape and orientation, δ is too small to measure ($<1\%$). Measurements of real rocket exhaust plumes are unlikely to achieve this level of precision in the near future, and so this parameter has been set to zero and ignored in our model.

The simple nonspherical shapes considered by the T-matrix code are obviously only a first approximation to the correct particle shape. In fact, they might be thought of as merely the leading term in an orthogonal series expansion of particle shape similar to spherical harmonics. However, Eq. (1) shows that if one is interested only in backscatter, then the precise details of particle shape do not necessarily matter. The only two observable parameters are the net backscatter intensity S_{11} and the depolarization Δ. Therefore, even if they do not reproduce the actual shape of a rocket particle, any distribution of "best-fit" ellipsoid or Chebyshev particle that reproduces the correct values of S_{11} and Δ will also reproduce all of the observable backscatter features of the actual exhaust plume. Additional justification of this point of view is provided by Kahnert et al.,[24] who concluded that the diagonal elements of the scattering matrix for complex particle shapes can be accurately reproduced by distributions of spheroids.

We first calculated a raw database of scattering parameters S_{11} and Δ spanning the relevant ranges of particle sizes and shapes, and then attempted to curve fit these results to develop a simple model suitable for use in backscatter calculations. Figures 4 and 5 summarize the computational database. These plots contain calculations for several thousand T2 Chebyshev and spheroidal particles with radii between 0.1 to $\cong 6$ μm and for nonsphericities ε between with $-0.4 < \varepsilon < +0.4$. Figure 4 shows the normalized values of S_{11}, that is, divided by the backscatter cross section of an equivalent volume sphere S_{11} (sphere). These normalized S_{11} values start off near unity for small particles and decreases more or less monotonically with increasing particle radius. The falloff is more abrupt for more nonspherical particles. Figure 5 shows a similar plot for the depolarization factor Δ. Because the depolarization of a sphere is zero,

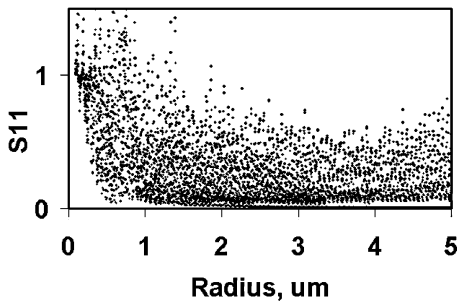

Fig. 4 Raw intensity database.

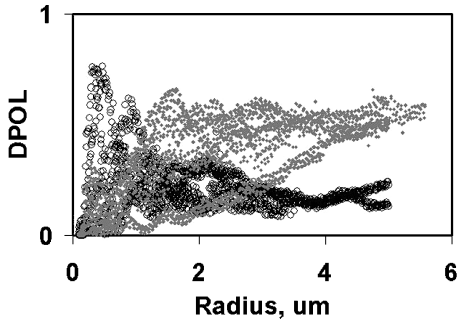

Fig. 5 Raw polarization database.

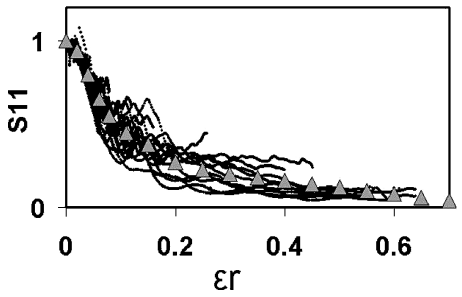

Fig. 6 Correlated intensity data.

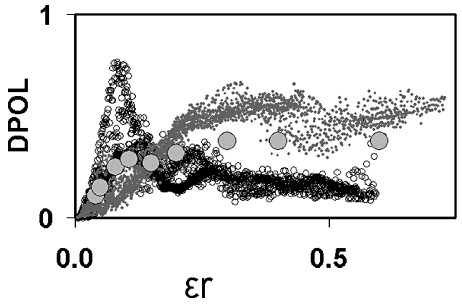

Fig. 7 Correlated polarization data.

these values are not normalized in any way. The significant point is that there is strong depolarization even for relatively small deviations from spherical shape. Note also that unlike the normalized values of S_{11}, the depolarization Δ is not monotonic with respect to particle size.

In an effort to identify some underlying regularity in Figs. 4 and 5, we first smoothed the fine-scale interference structure of the backscatter from the equivalent volume sphere in order to get better behaved ratios of the normalized backscatter cross-section ratios S_{11}/S_{11} (sphere). The smoothed normalized S_{11} ratios were then replotted with a new abscissa equal to $|\varepsilon r|$. This is heuristically motivated by the fact that the phase mismatch between various ray paths within the particle should scale with $(n-1)\varepsilon r/\lambda$, where n is the refractive index and λ is the wavelength. When replotted in this fashion, the normalized backscatter cross sections S_{11} cluster along a fairly narrow band (Fig. 6) with centroid denoted by $\Phi(\varepsilon r)$. The reader is cautioned that this approximate scaling relation with respect to $|\varepsilon r|$ is a fortunate happenstance and not a general result. It does not apply, for example, to small Rayleigh-sized particles, nor does it apply to refractive indexes significantly different from $m \cong 1.75$ (e.g., Ref. 25).

When the same $|\varepsilon r|$ coordinate transformation is applied to the depolarization data, the polarizations separate into two distinct branches corresponding to prolate and oblate particles (Fig. 7). In this figure, the fine-scale interference structure was not smoothed over. Whereas the polarization of the prolate particles (open circles) exhibits an initial rise and overshoot, the polarization of oblate ones (dots) tends to increase more smoothly and monotonically. For both types, the depolarization saturates for $|\varepsilon r| > 0.3$ and shows little change for larger values. However, the saturation levels are different for the two shapes. Because rocket exhaust particles are assumed to favor neither shape, we have averaged the two branches of the curve together to obtain a median curve $\Delta(\varepsilon r)$ denoted by the large dots in Fig. 7. Tables 1 and 2 give interpolation tables for $\Phi(\varepsilon r)$ and $\Delta(\varepsilon r)$. Because the nominal value for $|\varepsilon r|$ is approximately ≈ 0.1 for typical rockets, the span of $|\varepsilon r|$ in these tables covers the range of interest.

The backscatter from particles in a rocket exhaust plume involves a weighted average over both the size distribution $g(r)$ and shape distribution $f(\varepsilon)$. The intensity of the backscatter for particles of radius r, $\sigma_B(r)$, relative to the value predicted for an ideal sphere by

Table 1 $\Phi(\varepsilon r)$

εr	Φ	εr	Φ
0.00	1.00	0.35	0.18
0.02	0.94	0.40	0.16
0.04	0.80	0.45	0.14
0.06	0.65	0.50	0.12
0.08	0.55	0.55	0.10
0.11	0.45	0.60	0.08
0.15	0.38	0.65	0.06
0.20	0.27	0.70	0.04
0.25	0.23	0.75	0.02
0.30	0.20	10.00	0.00

Table 2 $\Delta(\varepsilon r)$

εr	Δ	εr	Δ
0.00	0.00	0.11	0.29
0.04	0.11	0.15	0.27
0.05	0.15	0.20	0.32
0.08	0.25	0.30	0.38

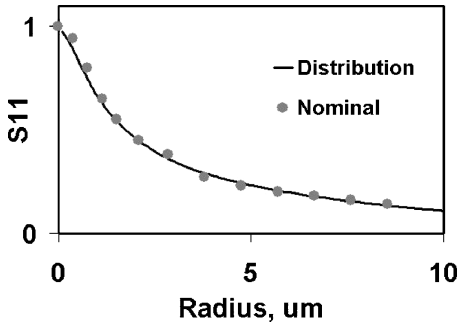

Fig. 8 Mean nonsphericity for intensity.

Mie theory, is

$$\frac{\sigma_B(r)}{\sigma_{\mathrm{MIE}}(r)} = \int \Phi(\varepsilon r) f(\varepsilon)\, \mathrm{d}\varepsilon \tag{2}$$

Performing a numerical integration with the measured $f(\varepsilon)$ distribution shown in Fig. 2, one obtains the solid curve in Fig. 8. Compared to equivalent volume spheres, the backscatter efficiency of rocket particles decreases monotonically with increasing particle radius. Figure 8 shows that to good approximation one can replace the integral of Eq. (2) by a one-point quadruture corresponding to a weighted mean value of $\varepsilon = 0.0526$.

$$\int \Phi(\varepsilon r) f(\varepsilon)\, \mathrm{d}\varepsilon \cong \Phi(0.0526 \cdot r) \tag{3}$$

Thus, the backscatter for an ensemble of particles in an exhaust plume can be recast into a form similar to that used by conventional Mie theory, with the addition of a correction term equal to $\Phi(0.0526r)$.

$$\sigma_B \cong \int \sigma_{\mathrm{MIE}}(r)\Phi(0.0526r) g(r)\, \mathrm{d}r \tag{4}$$

As a sample application of the backscatter model, we consider the recent WB-57F particle collection from a Titan-IVA plume, Fig. 9 (from Ref. 13). For this specific particle size distribution, the predictions of the present model are compared to those of conventional Mie theory in Table 3. The units for the backscatter intensity are arbitrary, but the same units are used for both the Mie and T-matrix columns. Also included are predictions of the logarithmic derivatives of both the intensity and depolarization with respect to wavelength. These are commonly used in lidar measurements because they are independent of the absolute calibration of the system.[26] The importance

Table 3 Predicted Titan-IVA properties

Parameter	Mie	T-matrix
σ_B (355)	3.72	1.60
σ_B (532)	2.52	1.38
σ_B (1064)	1.22	0.95
Δ (355)	0	0.27
Δ (532)	0	0.24
Δ (1064)	0	0.12
$-\mathrm{d}\ell_n(\sigma_B)/\mathrm{d}\ell_n\lambda$	1.02	0.48
$-\mathrm{d}\ell_n(\Delta)/\mathrm{d}\ell_n\lambda$	N/A	0.55

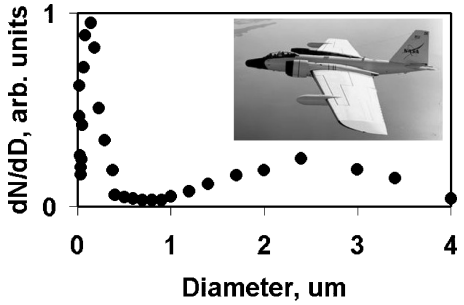

Fig. 9 Titan IVA particle size distribution.

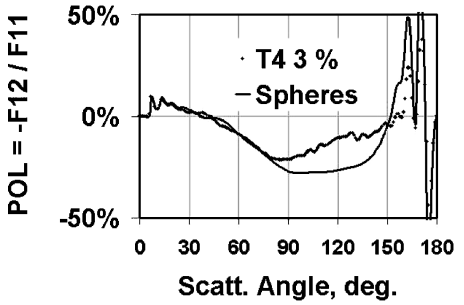

Fig. 10 Polarization of solar scattering.

of modeling nonsphericity varies according to wavelength and the specific parameter of interest. Table 3 suggests that the assumption of spherical particles results in an overestimation of near UV plume backscatter intensity by nearly a factor of two. Ross et al.[13] used a 785-nm laser particle counter and Mie theory to measure particle size in the Titan IVA plume. If, as we propose, Mie theory is not appropriate for such particles, then Ross et al. could overestimate the particle sizes by tens of percent. Our main conclusions remain, however, and the differences between the Mie and T-matrix predictions in Table 3 are significant enough to warrant consideration by those performing laser-based plume measurements (i.e., lidar or particle counters) or proposing such systems. In addition, our results suggest the need for reanalysis of existing data in cases where the details of the alumina size distribution are important.[10,27]

Because nonspherical particles typically exhibit a characteristic polarization signature, we have also investigated what one might learn from simple polarization measurements of scattered sunlit from missile contrails. Figure 10 compares the predicted polarization for a log-normal distribution (center radius $= 2.5$ μm and geometric standard deviation $= 1.07$) of spheres vs Chebyshev T4 particles with $\varepsilon = 3\%$ nonsphericity. Significant differences are noted near scattering angles of $\approx$120 deg. This preliminary result indicates that such polarization measurements can provide useful information about particle shape. However, the problem of retrieving reliable shape information in cases where the particle size distribution is not known a priori requires further investigation.

IV. Summary

We have attempted to define a procedure whereby one might make improved estimates of the backscatter from Al_2O_3 rocket exhaust particles by taking account of the slight nonsphericity observed in various collected samples. Based upon the observed shape distribution and the T-matrix code of Mishchenko et al. for nonspherical particles, we expect the lidar cross section of rocket particles to be significantly less than predicted by Mie theory for size parameters in excess of 10 (i.e., about 1-μm radius at 532-nm wavelength). We also expect significant differences in the wavelength slope of the lidar intensity $\mathrm{d}\ell_n(\sigma)/\mathrm{d}\ell_n(\lambda)$.

These calculations do not consider the precise shape of the particles, nor do they consider the additional effects of internal inhomogeneities in the particles such as voids, cracks, and grain boundaries, which are apparent in the scanning electron microscope photographs of some particles. However, as Eq. (1) shows, the only observables in the precise backscatter direction are the overall intensity S_{11} and the depolarization Δ. Thus, any particle shape that reproduces the correct values for these two parameters, even if it does not reproduce the actual shape of a rocket particle, will reproduce the observable backscatter properties of the exhaust plume. Condensation of water and acids in low-altitude rocket exhaust plumes can lead to additional modifications of the plume backscatter that are not considered here. This should be taken into account in any backscatter measurement of contrails where condensation has had time to occur.[3] Last, although one can imagine numerous refinements to the model, we feel that further development is premature and should be deferred until such a time as it can be calibrated against actual plume lidar data.

Acknowledgments

We thank J. Wesley Cofer of NASA Langley Research Center and P. Kessel and M. Holmes of the U.S. Air Force Research Laboratory (AFRL) for providing additional rocket particle scanning electron microscope photomicrographs. We also acknowledge M. Wheling and M. Venner of AFRL and J. Stryjewski of the Innovative Science Technology Experimentation Facility.

References

[1]Christou, C. T., and Levin, D. A., "Analysis of Laser Backscattering from Solid Fuel Rocket Plumes," *AIAA Journal*, Vol. 29, No. 8, 1991, pp. 1259–1265.

[2]Beiting, E. J., "Solid Rocket Exhaust Model for Alumina Particles in the Stratosphere," *Journal of Spacecraft and Rockets*, Vol. 34, No. 3, 1997, pp. 303–310.

[3]Beiting, E. J., "Predicted Optical Characteristics of Solid Rocket Motor Exhaust in the Stratosphere," *Journal of Spacecraft and Rockets*, Vol. 34, No. 3, 1997, pp. 311–317.

[4]Dentamaro, A. V., Dao, P. D., Farley, R., and Ross, M., "Characterization of Particles from Stratospheric Launch Vehicle Plumes Using Wavelength-Dependant Lidar Techniques," *Geophysical Research Letters*, Vol. 26, No. 15, 1999, pp. 2395–2398.

[5]Zolensky, M. E., "The Abundance and Origin of Aluminum-Rich Particulates in the Stratosphere," *EOS, Transactions of the American Geophysical Union*, Vol. 65, 1984, p. 837.

[6]Zolensky, M. E., and Mackinnon, I. D. R., "Accurate Stratospheric Particle Size Distributions from a Flat-Plate Collection Surface," *Journal of Geophysical Research*, Vol. 90, No. D3, 1985, pp. 5801–5808.

[7]Zolensky, M. E., McKay, D. S., and Kaczor, L. A., "A Ten-Fold Increase in the Abundance of Large Solid Particles in the Stratosphere, as Measured over the Period 1976–1984," *Journal of Geophysical Research*, Vol. 94, No. D1, 1989, pp. 1047–1056.

[8]Thomas-Ver Ploeg, K. L., and Zolensky, M. E., "A Comparison of Shuttle Solid Rocket Effluent with Aluminum-Rich Stratospheric Particles," *EOS, Transactions of the American Geophysical Union*, Vol. 66, 1985, p. 826.

[9]Ross, M. N., and Zittel, P. F., "Study Blazing New Trails into the Effects of Aviation and Rocket Exhaust in the Atmosphere," *EOS Transactions*, Vol. 80, 1999, pp. 437–443. URL: http://www.aero.org/publications/crosslink/summer2000/01.html.

[10]Gates, A. M., Avallone, L. M., Tookey, D. W., Rutter, A. P., Whitefield, P. D., Hagan, D. E., Hopkins, A. R., Ross, M. N., Zittel, P. F., Thompson, T. L., Herman, R. L., and Friedl, R. R., "In Situ Measurements of Carbon Dioxide, 0.37-4.0 μm Particles, and Water Vapor in the Stratospheric Plumes of Small Rockets," *Journal of Geophysical Research*, Vol. 107, No. D22, 2002, p. 4649.

[11]Murphy, P. J., Reed, R. A., Cox, D. B., Wilcher, G. A., Watkins, W. A., Truesdale, R., Simmons, M. A., and Roberds, D. W., "Measurement and Analysis of Laser Transmission Through Solid-Propellant Rocket Motor Exhaust Plumes," AIAA Paper 93-2886, July 1993.

[12]Hermsen, R. W., "Aluminum Oxide Particle Size for SRM Performance Prediction," *Journal of Spacecraft and Rockets*, Vol. 18, No. 6, 1981, pp. 483–490.

[13]Ross, M. N., Whitefield, P. D., Hagen, D. E., and Hopkins, A. R., "In Situ Measurement of the Aerosol Size Distribution in Stratospheric Solid Rocket Motor Exhaust Plumes," *Geophysical Research Letters*, Vol. 26, No. 7, 1999, pp. 819–822.

[14]Reed, R. A., and Calia, V. S., "Review of Aluminum Oxide Rocket Exhaust Particles," AIAA Paper 93-2819, July 1993.

[15]Dill, K., Reed, R. A., Schulz, R. J., and Calia, V. S., "Crystalline Phase Analysis of Aluminum Oxide (Al2O3) Captured from Solid Propellant Rocket Exhaust Particles," *Journal of Propulsion and Power*, Vol. 6, No. 5, 1990, pp. 668–671.

[16]Oliver, S. M., and Reed, R. A., "The Kinetics of Alpha vs. Gamma Al2O3 Particle Formation in Solid Propellant Rocket Exhausts," AIAA Paper 91-0380, Jan. 1991.

[17]Mishchenko, M. I., and Travis, L. D., "Capabilities and Limitations of a Current FORTRAN Implementation of the T-Matrix Method for Randomly Oriented, Rotationally Symmetric Scatterers," *Journal of Quantitative Spectroscopy and Radiative Transfer*, Vol. 60, No. 3, 1998, pp. 309–324. URL: http://www.giss.nasa.gov/∼crmim/t_matrix.html.

[18]Bohren, C. F., and Huffman, D. R., *Absorption and Scattering of Light by Small Particles*, Wiley, New York, 1983, Chap. 13.

[19]Mishchenko, M. I., Hovenier, J. W., and Travis, L. D., *Light Scattering by Nonspherical Particles*, Academic Press, San Diego, CA, 2000, Chap. 4.

[20]Mishchenko, M. I., and Travis, L. D., "Electromagnetic Scattering by Nonspherical Particles," *Exploring the Atmosphere by Remote Sensing*, edited by R. Guzzi, Springer-Verlag, Heidelberg, Germany, 2003, pp. 77–127.

[21]Volten, H., Jalava, J. P., Lumme, K., de Haan, J. F., Vassen, W., and Hovenier, J. W., "Laboratory Measurements and T-Matrix Calculations of the Scattering Matrix of Rutile Particles in Water," *Applied Optics*, Vol. 38, No. 24, 1999, pp. 5232–5240.

[22]Munoz, O., Volten, H., de Haan, J. F., Vassen, W., and Hovenier, J. W., "Experimental Determination of Scattering Matrices of Olivine and Allende Meteorite Particles," *Astronomy and Astrophysics*, Vol. 360, Aug. 2000, pp. 777–788.

[23]Hovenier, J. W., "Measuring Scattering Matrices of Small Particles at Optical Wavelengths," *Light Scattering by Nonspherical Particles*, edited by M. I. Mishchenko, J. W. Hovenier, and L. D. Travis, Academic Press, New York, 2000, pp. 355–365.

[24]Kahnert, F. M., Stamnes, J. J., and Stamnes, K., "Using Simple Particle Shapes to Model the Stokes Scattering Matrix of Wavelength-Sized Particles with Complex Shapes: Possibilities and Limitations," *Journal of Quantitative Spectroscopy and Radiative Transfer*, Vol. 74, No. 2, 2002, pp. 167–182.

[25]Mishchenko, M. I., Travis, L. D., and Mackowski, D. W., "T-Matrix Computations of Light Scattering by Nonspherical Particles: A Review," *Journal of Quantitative Spectroscopy and Radiative Transfer*, Vol. 55, No. 5, 1996, pp. 535–575.

[26]Mishchenko, M. I., and Sassen, K., "Depolarization of Lidar Returns by Small Ice Crystals: an Application to Contrails," *Geophysical Research Letters*, Vol. 25, No. 3, 1998, pp. 309–312.

[27]Ross, M. N., and Friedl, R. F., "The Impact of Solid and Liquid Propellant Rocket Engine Emissions on Stratospheric Ozone: Results from RISO and ACCENT Plume Measurement Programs," *Proceedings of the 6th International Symposium on Propulsion for Space Transportation for the 21st Century*, Versailles, France, 2002.

A. Ketsdever
Associate Editor